Analysis of Huygens metasurface for transmit-reflect array design

Alessio Berto, Francesco Foglia Manzillo, Guido Valerio

Analysis of Huygens' Metasurfaces for the Design of Transmit-Reflect Arrays

Alessio Berto * † , Francesco Foglia Manzillo *, and Guido Valerio †,
*CEA - Leti, Univ. Grenoble Alpes, F-38000 Grenoble, France,
{alessio.berto, francesco.fogliamanzillo}@cea.fr
†Sorbonne Université, CNRS, Laboratoire de Génie Electrique et Electronique de Paris (GeePs), 75252, Paris, France
Université Paris-Saclay, CentraleSupélec, CNRS, GeePs, 91192, Gif-sur-Yvette, France
guido.valerio@sorbonne-universite.fr

***Abstract*—In this article, we propose a rigorous approach to determine the surface parameters of Huygens' metasurface cells for the design of high-efficiency transmit-reflect arrays. We demonstrate that the power of a normally incident plane wave can be evenly split into the transmitted and reflected ones, and that, at the same time, arbitrary phase shifts can be introduced on the scattered waves. As a proof of concept, four cells realizing a uniform 2-bit quantization of the phase range, in transmission and reflection, are designed. Each cell comprises two dielectric slabs and three impedance sheets which are derived from the optimal surface parameters. Moreover, the bandwidth performance are preliminarily assessed.**

***Index Terms*—transmit-reflect array, field transformations, metasurfaces, wavefront manipulation.**

I. Introduction

In the last decade, a lot of attention has been directed to metasurfaces, engineered 2-D structures composed of electrically small unit cells [1], [2]. They are often realized using stacked patterned layers with cells equally spaced at subwavelength distances. Due to the small size of cells, a metasurface can be modeled, in general, as a homogeneous sheet characterized by tensors describing its electric, magnetic and magneto-electric responses.

The capability of tailoring reflected and transmitted waves, when illuminated by an incident wavefront, has been leveraged in diverse low-profile devices, such as reflectionless lenses [3], reflective intelligent surfaces (RIS) [4], from microwave to optical frequencies. Metasurfaces are effective solutions for the design of high-efficiency and compact spatially fed arrays antennas, like transmitarrays (TAs) or reflectarrays (RAs) that, contrarily to conventional arrays, do not require complex feeding networks. A promising device that has been recently proposed is the transmit-reflect array (TRA), that provides both RA and TA functionalities. However, most TRA designs are based on full-wave parametric optimizations of the geometries of the unit cells. Moreover, they often reflect and transmit waves with different polarizations or at different frequencies [5]–[8].

In this paper, we present a rigorous procedure to design Huygens' metasurface unit cells with applications to TRAs. We show that it is possible to cover the full-phase range both in transmission and reflection maintaining an even division of the incident power. We analytically determine the constitutive parameters of the cells and present a preliminary design of the TRA cells with a three-layer structure. The bandwidth performance are investigated.

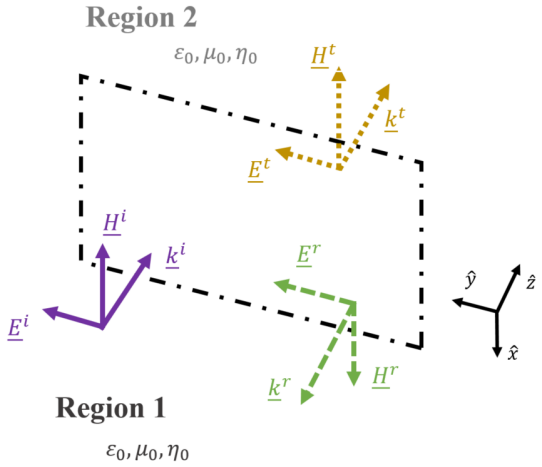

Fig. 1. Infinite Huygens' metasurface between two regions with the same material properties, illuminated by a normal incident field, in purple line. Reflected and transmitted fields are in green and yellow lines, respectively.

II. Analysis under Normal Incidence

We will consider a non-chiral, lossless and isotropic metasurface that exhibits both electric and magnetic response but no magneto-electric one. The structure is illuminated by a normally incident plane wave polarized along $\hat{y}$, as shown in Fig. 1.

Assuming the metasurface as a homogeneous and infinitesimally thin structure, the induced surface currents can be related to the average tangential fields on the surface [9], [10]:

$$\begin{pmatrix} \underline{J}_s \\ \underline{M}_s \end{pmatrix} = \begin{pmatrix} Y_e \bar{\bar{I}} & 0 \\ 0 & Z_m \bar{\bar{I}} \end{pmatrix} \begin{pmatrix} \underline{E}_{t,avg} \\ \underline{H}_{t,avg} \end{pmatrix}, \qquad (1)$$

where the average fields tangent to the surface are defined as $\underline{E}_{t,avg} = 1/2\left(\underline{E}^i + \underline{E}^r + \underline{E}^t\right)$ and $\underline{H}_{t,avg} = 1/2\left(\underline{H}^i + \underline{H}^r + \underline{H}^t\right)$. Moreover, due to the lossless condition, the electric admittance is $Y_e = jB_e$ and the magnetic impedance is $Z_m = jX_m$, with B_e and X_m real.

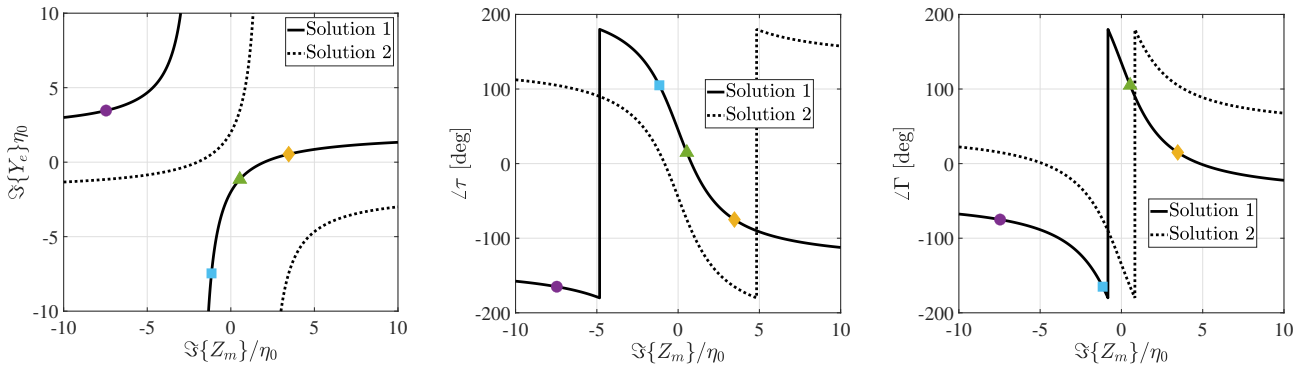

(a) (b) (c)

Fig. 2. (a) Loci of (Z_m, Y_e) for which $|\tau| = |\Gamma|$. Two separate solutions are found. Phase of the (b) transmission and (c) reflection coefficients, obtained for these solutions.

By virtue of the equivalence principle, the following boundary conditions are derived:

$$\underline{J}_s = \hat{z} \times \hat{x}\,(H_2 - H_1) = \hat{y} Y_e E_{t,avg}\,, \tag{2}$$

$$\underline{M}_s = -\hat{z} \times \hat{y}\,(E_2 - E_1) = \hat{x} Z_m H_{,avg}\,, \tag{3}$$

where $\underline{H}_1 = (H^r - H^i)\hat{x}$, $\underline{H}_2 = -H^t\hat{x}$, $\underline{E}_1 = (E^i + E^r)\hat{y}$ and $\underline{E}_2 = E^t\hat{y}$.

We define the transmission and reflection coefficients as the ratios of the transmitted and reflected wave, respectively, to the incident one: $\tau = E^t/E^i$ and $\Gamma = E^r/E^i$. From (2) and (3), after some manipulations, the following expressions for Γ and τ are found:

$$\Gamma = \frac{Z_m - Y_e\eta_0^2}{2\eta_0\left(1 + \dfrac{Y_e\eta_0}{2}\right)\left(1 + \dfrac{Z_m}{2\eta_0}\right)}\,, \tag{4}$$

$$\tau = \frac{1 - \dfrac{Z_m Y_e}{4}}{\left(1 + \dfrac{Y_e\eta_0}{2}\right)\left(1 + \dfrac{Z_m}{2\eta_0}\right)}\,, \tag{5}$$

where η_0 is the free-space characteristic impedance.

A. Condition for Equal Transmission and Reflection

It has been demonstrated that Huygens' metasurfaces can achieve a perfect transmission or reflection [3].

We focus here on the possibility of evenly split the incident power into the transmitted and reflected field, as well as on the maximum achievable phase-shift range in transmission and reflection.

To this end, we enforce the following condition and solve it for Y_e and Z_m:

$$|\tau(Z_m, Y_e)| = |\Gamma(Z_m, Y_e)|\,. \tag{6}$$

Using (4) and (5), two solutions are found, which stipulate the following relationships between B_e and X_m:

$$B_{e_1} = \frac{2X_m - 4\eta_0}{2\eta_0^2 + \eta_0 X_m}\,, \tag{7}$$

$$B_{e_2} = \frac{2X_m + 4\eta_0}{2\eta_0^2 - \eta_0 X_m}\,. \tag{8}$$

The loci of admittances and impedances in (7) and (8) are plotted in Fig. 2(a). The phases of τ and Γ obtained for these two solutions are shown in Fig. 2(b) and Fig. 2(c), respectively. They vary in the entire $360°$ range, enabling the realization of TRAs with arbitrary phase profiles in transmission or in reflection.

However, it can be observed that the differences between $\angle\tau$ and $\angle\Gamma$ obtained with the first and second solution are equal to $-90°$ and $90°$, respectively.

Therefore, $\angle\tau$ and $\angle\Gamma$ cannot be controlled separately: by setting one, the second is directly defined. In a practical TRA design, this means that by setting the direction for the beam in transmission, the beam direction in reflection is automatically defined.

III. Preliminary TRA Cell Design

As a proof of concept, we propose a preliminary design of four unit cells of a TRA realizing a uniform 2-bit quantization of the full phase range. It has already been demonstrated that with this number of bits, the directivity loss due to quantization is around 1 dB, without a significant degradation of the scanning performance [11].

The selected phases ϕ_τ of the transmission coefficients of the cells and the corresponding values of electric admittance and magnetic impedance, chosen from the first solution for $|\tau| = |\Gamma|$, are reported in Table I, and shown with markers in Fig. 2.

We choose to design the metasurface cells using three impedance sheets interleaved by two dielectric slabs, as shown in Fig. 3. As proved in [9], [12], the outer impedance sheets of a three-layer Huygens' metasurface are equal.

The Huygens' metasurface can be modeled as a two-port network. The entries of its symmetric impedance matrix are linked to the surface parameters Y_e, Z_m as follows [9], [12]:

TABLE I
IMPEDANCE SHEET VALUES FOR A 2 BIT TRA

ϕ_τ [deg]	$\Im(Z_m)/\eta_0$	$\Im(Y_e)\eta_0$	$\Im(Z_{s_1})$ [Ω]	$\Im(Z_{s_2})$ [Ω]
15	0.54	-1.16	167.52	-2128.53
105	-1.16	-7.46	-117.17	-82.31
195	-7.46	3.46	-215.13	123.76
285	3.46	0.54	-415.87	50.61

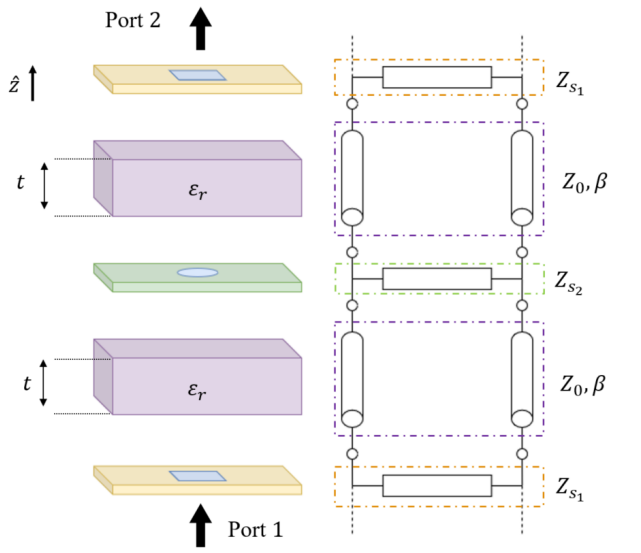

Fig. 3. Geometry and equivalent circuit model of the TRA unit cell comprising the sheet impedances.

$$\begin{pmatrix} Z_{11} & Z_{12} \\ Z_{21} & Z_{22} \end{pmatrix} = \begin{pmatrix} \frac{1}{Y_e} + \frac{Z_m}{4} & \frac{1}{Y_e} - \frac{Z_m}{4} \\ \frac{1}{Y_e} - \frac{Z_m}{4} & \frac{1}{Y_e} + \frac{Z_m}{4} \end{pmatrix} \tag{9}$$

The values of the impedance sheets Z_{s_1} and Z_{s_2} of the proposed three-layer structure of Fig. 3 can be found using the following formulas [12]:

$$Z_{s_1} = \frac{Z_0 \tan(\beta t)}{j + Z_0 \tan(\beta t) \dfrac{Z_{11} + Z_{12}}{Z_{11}^2 - Z_{12}^2}}, \tag{10}$$

$$Z_{s_2} = -\frac{[Z_0 \tan(\beta t)]^2 \dfrac{Z_{12}}{Z_{11}^2 - Z_{12}^2}}{\sec(\beta t)^2 - 2jZ_0 \tan(\beta t) \dfrac{Z_{12}}{Z_{11}^2 - Z_{12}^2}}, \tag{11}$$

where Z_0 is the characteristic impedance in the slab, t is the thickness of a single slab, $\beta = 2\pi/\lambda_0\sqrt{\epsilon_r}$ is the propagation constant in the dielectric, which has a relative permittivity ϵ_r, and λ_0 is the free-space operating wavelength.

For the design of the cells, we choose a slab permittivity $\epsilon_r = 2.2$, a thickness $t = \lambda_g/8$, where $\lambda_g = \lambda_c/\sqrt{\epsilon_r}$ and λ_c is the free-space wavelength at the design frequency $f_c = 30$ GHz. With these parameters, using (10) and (11), the pairs of impedance sheets Z_{s_1} and Z_{s_2} shown in Table I are found for the four TRA cells.

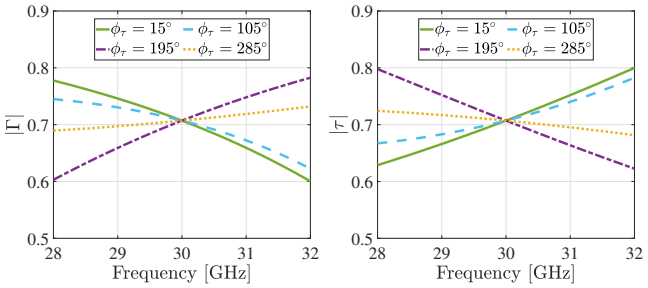

Fig. 4. Magnitudes of the (a) reflection and (b) transmission coefficients of the TRA cells as functions of frequency.

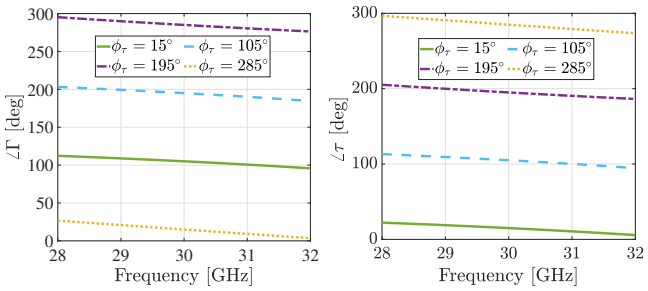

Fig. 5. Phases of the (a) reflection and (b) transmission coefficients of the TRA cells as functions of frequency.

We now compute the scattering parameters of the designed unit cells as functions of frequency, using the transfer-matrix approach [3] and the equivalent circuit of Fig. 3. The values of Z_{s_1} and Z_{s_2} are considered constant with respect to the frequency. We analyze the impact of frequency dispersion introduced by the slabs in the range $28 - 32$ GHz. The frequency behaviour of $|\tau|$ and $|\Gamma|$ are reported in Fig. 4. In a 13% relative bandwidth, the variation in the amplitude of both τ and Γ is only ± 0.5 dB, with respect to their values at the central frequency of 30 GHz.

The phases of reflection and transmission coefficients of the four cells are plotted versus frequency in Fig. 5. It can be noticed that at 30 GHz, the phases are spaced by exactly 90°. In the considered frequency range, the maximum relative phase error is 8°.

IV. Conclusion

We have demonstrated that a Huygens' metasurface can evenly split the power of a normally incident field into the reflected and transmitted wave, while introducing an arbitrary phase shift to select the direction of the transmitted wave, which in turn fixes the direction of the reflected wave. The surface parameters enabling these functionalities have been analytically determined. As proof of concept, four TRA unit cells achieving a uniform 2-bit quantization in both reflection and transmission have been designed using three impedance

sheets and two dielectric slabs. The scattering parameters of the four cells have been computed for frequency-independent impedance sheets using the transfer-matrix approach. It has been shown that these cells operate over a 13% relative bandwidth with a maximum variation of ± 0.5 of the magnitudes of both reflection and transmission coefficient. These results pave the way for the realization of TRAs by using metasurfaces constituted of suitable periodic patterns of printed metallic elements capable to simulate the desired impedance sheets in the required band.

REFERENCES

[1] C. L. Holloway, E. F. Kuester, J. A. Gordon, J. O'Hara, J. Booth, and D. R. Smith, "An overview of the theory and applications of metasurfaces: The two-dimensional equivalents of metamaterials," *IEEE Antennas Propag. Mag.*, vol. 54, no. 2, pp. 10–35, Feb. 2012.

[2] E. Martini and S. Maci, "Modulated metasurfaces for microwave field manipulation: Models, applications, and design procedures," *IEEE J. Microwaves*, vol. 2, no. 1, pp. 44–56, Jan. 2022.

[3] C. Pfeiffer and A. Grbic, "Metamaterial huygens' surfaces: Tailoring wave fronts with reflectionless sheets," *Phys. Rev. Lett.*, vol. 110, pp. 1–5, May 2013.

[4] V. Degli-Esposti, E. M. Vitucci, M. Di Renzo, and S. Tretyakov, "Reradiation and scattering from a reconfigurable intelligent surface: A general macroscopic model," *IEEE Trans. Antennas Propag.*, vol. 70, no. 10, pp. 8691–8706, Oct. 2022.

[5] X. Liu, Z. Yan, E. Wang, X. Zhao, T. Zhang, and F. Fan, "Dual-band orthogonally-polarized dual-beam reflect-transmit-array with a linearly polarized feeder," *IEEE Trans. Antennas Propag.*, vol. 70, no. 9, pp. 8596–8601, Sept. 2022.

[6] S. Liu and Q. Chen, "A wideband, multifunctional reflect-transmit-array antenna with polarization-dependent operation," *IEEE Trans. Antennas Propag.*, vol. 69, no. 3, pp. 1383–1392, Mar. 2021.

[7] X. Li, Q. Huang, L. Yang, M. Cai, S. Yang, S. Yang, and Y. Li, "Dual-band wideband reflect-transmit-array with different polarizations using three-layer elements," *IEEE Antennas Wirel. Propag. Lett.*, vol. 20, no. 7, pp. 1317–1321, Jul. 2021.

[8] Z. H. Jiang, F. Wu, X. W. Zhu, Q. Ren, P. L. Werner, and D. H. Werner, "Metasurface-based circularly-polarized multibeam reflect-transmit-arrays," in *Proc. 14^{th} Eur. Conf. Antennas Propag. (EuCAP)*, Copenhagen, Denmark, Mar. 2020, pp. 1–3.

[9] A. Epstein and G. V. Eleftheriades, "Huygens' metasurfaces via the equivalence principle: design and applications," *J. Opt. Soc. Am.*, vol. 33, no. 2, pp. A31–A50, Feb. 2016.

[10] L. Szymanski, B. O. Raeker, C.-W. Lin, , and A. Grbic, "Fundamentals of lossless, reciprocal bianisotropic metasurface design," *Photonics*, vol. 8, no. 6, p. 197, Jun. 2021.

[11] H. Yang, F. Yang, S. Xu, M. Li, X. Cao, J. Gao, and Y. Zheng, "A study of phase quantization effects for reconfigurable reflectarray antennas," *IEEE Antennas Wirel. Propag. Lett.*, vol. 16, pp. 302–305, May 2017.

[12] A. Epstein and G. V. Eleftheriades, "Arbitrary power-conserving field transformations with passive lossless omega-type bianisotropic metasurfaces," *IEEE Trans. Antennas Propag.*, vol. 64, no. 9, pp. 3880–3895, Sept. 2016.